Cancer Chemother Pharmacol (2011) 68:513–524
DOI 10.1007/s00280-010-1518-3

ORIGINAL ARTICLE

Preclinical pharmacokinetics, metabolism, and toxicity of azurin-p28 (NSC745104) a peptide inhibitor of p53 ubiquitination

Lee Jia · Gregory S. Gorman · Lori U. Coward · Patricia E. Noker · David McCormick · Thomas L. Horn · J. Brooks Harder · Miguel Muzzio · Bellur Prabhakar · Balaji Ganesh · Tapas K. Das Gupta · Craig W. Beattie

Received: 9 September 2010 / Accepted: 29 October 2010 / Published online: 18 November 2010

Abstract
Purpose Characterize the preclinical pharmacokinetics, metabolic profile, multi-species toxicology, and antitumor efficacy of azurin-p28 (NSC 745104), an amphipathic, 28 amino acid fragment (aa 50–77) of the copper containing redox protein azurin that preferentially enters cancer cells and is currently under development for treatment of p53-positive solid tumors.
Methods An LC/MS/MS assay was developed, validated, and applied to liver microsomes, serum, and tumor cells to assess cellular uptake and metabolic stability. Pharmacokinetics was established after administration of a single intravenous dose of p28 in preclinical species undergoing chronic toxicity testing. Antitumor efficacy was assessed on human tumor xenografts. A human therapeutic dose was predicted based on efficacy and pharmacokinetic parameters.
Results p28 is stable, showed tumor penetration consistent with selective entry into tumor cells and significantly inhibited p53-positive tumor growth. Renal clearance, volume of distribution, and metabolic profile of p28 was relatively similar among species. p28 was non-immunogenic and non-toxic in mice and non-human primates (NHP). The no observed adverse effect level (NOAEL) was 120 mg/kg iv in female mice. A NOAEL was not established for male mice due to decreased heart and thymus weights that was reversible and did not result in limiting toxicity. In contrast, the NOAEL for p28 in NHP was defined as the highest dose (120 mg/kg/dose; 1,440 mg/m^2/dose) studied. The maximum-tolerated dose (MTD) for subchronic administration of p28 to mice is >240 mg/kg/dose (720 mg/m^2/dose), while the MTD for subchronic administration of p28 to *Cynomolgous* sp. is >120 mg/kg (1,440 mg/m^2/dose). The efficacious (murine) dose of p28 was 10 mg/kg ip per day.
Conclusions p28 does not exhibit preclinical immunogenicity or toxicity, has a similar metabolic profile among species, and is therapeutic in xenograft models.

Keywords Azurin · p28 · Pharmacokinetics · Toxicology · Chemotherapeutic

L. Jia
Developmental Therapeutics Program,
National Cancer Institute, Bethesda, MD 20852, USA

G. S. Gorman · L. U. Coward
Samford University, Birmingham, AL 35229, USA

P. E. Noker
Southern Research Institute, Birmingham, AL 35205, USA

D. McCormick · T. L. Horn · J. B. Harder · M. Muzzio
IIT Research Institute, Chicago, IL, USA

B. Prabhakar · B. Ganesh
Department of Microbiology and Immunology,
UIC-COM, Chicago, IL, USA

T. K. Das Gupta · C. W. Beattie (✉)
CDG Therapeutics, Chicago, IL, USA
e-mail: cbeattie@uic.edu

Introduction

Azurin, a member of the cupredoxin family of copper containing, redox proteins preferentially penetrates human cancer cells and exerts cytostatic and cytotoxic (apoptotic) effects with no apparent activity on normal cells [5, 8, 9]. Amino acids 50–67 (p18) are a minimal motif or protein transduction domain (PTD) responsible for azurin's preferential entry into human cancer cells. Azurin-p28 (p28), amino acids 50–77 (NSC 745104), also preferentially enters human cancer cells and inhibits cancer cell

proliferation [7, 10]. These amphipathic, α-helical peptides are unique as they are not bound by cell membrane glycosaminoglycans and preferentially penetrate cancer cells via endocytotic, caveosome-directed, and caveosome-independent pathways [7]. p28 exerts its anti-proliferative activity by reducing proteasomal degradation of p53 through formation of a p28: p53 complex within a hydrophobic DNA-binding domain (aa 80–276), increasing p53 levels and DNA-binding activity [10]. Subsequent elevation of the cyclin-dependent kinase inhibitors p21 and p27 reduces CDK2 and cyclin A and produces a G2/M phase cell cycle arrest [10]. The significant reduction in proteasomal degradation of p53 through an MDM2-independent pathway(s) by p28 provides a lead into a unique series of cytostatic and cytotoxic (apoptotic) chemotherapeutic agents. Here, we present the preclinical pharmacokinetics, metabolism, toxicity, and in vivo efficacy of p28 and demonstrate its lack of immunogenicity.

Materials and methods

Materials

Azurin-derived p28 (Leu50-Asp77 LSTAADMQG VVTDGMASGLDKDYLKPDD, 2,914 Da) was synthesized by CS Bio, Inc. (Menlo Park, CA) at >95% purity and mass balance. p28 was provided as a white to off-white lyophilized powder in two lots, GC0413 (murine) and GC0911 (NHP), in pre-filled vials and stored at 4°C prior to use. MP-1 (Ac-SYGJEHfRWGKPV-NH2, where J = L-Norleucine and f = D-phenylalanine) as an internal standard was purchased from Mimotopes (Australia), HPLC grade acetonitrile, ammonium acetate, formic acid, and perchloric acid were purchased from Fisher Scientific (Atlanta, GA, USA), and formalin-free HIC Zinc fixative from BD Bioscience (San Jose, CA). Purified water was from a Millipore Milli-Q system (Bedford, MA). Serum was obtained from Lampire Biologics (Pipersville, PA). Pooled mouse, monkey, and human liver microsomes were purchased from Xenotech LLC (Lenexa, KS). Human cell line MDA-MB-231 (breast p53 mut) was obtained from ATCC (Manassas, VA), and HCT-116 (colon p53 wt) was a gift of Dr. B. Vogelstein, Johns Hopkins University. UISO-Mel-23 was developed and characterized in our laboratory [6]. Male athymic mice (Hsd:Athymic Nude-Foxn1nu; 4–5 weeks old) were purchased from Harlan Laboratories (Madison, WI), virus-free male and female CD-1 [Crl:CD1(ICR)] and BALB/c mice ~5 to 6 weeks old from Charles River Laboratories (Portage, MI). Male and female NHP *Cynomolgous* sp. 3–4 years old were from Covance Research Products (Alice, TX.). CD-1 mice and NHP were held in quarantine for a minimum of 6 weeks prior to randomization into experimental groups. All animals were certified as B-virus negative by the supplier, and each demonstrated two negative tuberculosis tests during the quarantine period. Protocols involving experimental animals were approved by the UIC and IIT Research Institute Animal Care and Use Committees in compliance with USDA regulations (National Research Council 1996). Toxicology and Pharmacokinetic studies were performed in fully accredited (AAALAC) laboratory facilities under current Good Laboratory Practice (cGLP) regulations following FDA guidelines and standard NCI protocols for preclinical toxicology studies of oncology drugs (http://www.fda.gov/cber/gdlns/canclin).

Methods

Analytical method

The analytical method [1] incorporated an HPLC system for sample separation (Perkin-Elmer, Norwalk, CT) with a series 200 autosampler, two micro-flow-rate pumps and an Aquasil C18 HPLC column (100 × 2 mm i.d., 5 μm particle size, Waltham, MA) protected with a Phenomenex C18 security guard cartridge. The mobile phase was delivered at a flow rate of 400 μl/min using a gradient elution profile consisting of 5 mM ammonium acetate with 0.5% formic acid (A) and acetonitrile with 0.5% formic acid (B). The starting mobile phase composition of 80% A/20% B was increased linearly to 5% A/95% B over a 3-min period after an initial 0.5 min hold, then held at 5% A/95% B for 1.5 min, and returned to 80% A/20% B (step gradient) and re-equilibrated for 2.5 min. An Applied BioSystems 4,000 QTrap (Toronto, Canada) triple quadrupole mass spectrometer operated in the positive ion mode was used for detection. The HPLC/MS/MS was equipped with an electrospray ion source operated at 450°C set at a potential of 5 kV with the orifice potential at 100 V. High purity nitrogen was used as the curtain and collision gas. Multiple reaction monitoring (MRM) was used to quantitate the following transitions: p28 (sum of *m/z* 972.4 → 1,236.3 and 972.4 → 1,272.3) and MP-1 (*m/z* 809.2 → 136.4). A dwell time of 150 ms was used for each ion transition. Collision energies were optimized for each transition and ranged from 40 eV for p28, to 95 eV for MP-1. Instrument control and quantitation were performed using Analyst 1.4 software (Applied Biosystems, Foster City, CA). The amount of p28 was back calculated using a calibration curve generated from a set of calibration standards (100–10,000 ng/ml, final concentrations) with correlation coefficients >0.99.

Stability

Formulations containing p28 at 2 or 50 mg/ml in 0.9% saline were stored for up to 96 h at 4°C and room

temperature and analyzed. Measured concentrations of p28 stored at room temperature ranged from 99 to 107% of the theoretical concentrations, indicating good stability for p28. The stability of p28 added to mouse, dog, non-human primate (NHP), or human serum at a final concentration of 10 and 100 μg ml^{-1} was analyzed as previously described [2]. The stability of p28 in pooled mouse, monkey, and human liver microsomes diluted to a final concentration of 1 mg/ml was determined using an NADPH regenerating system (BD Gentest, Woburn, MA) of 1.3 mM nicotinamide adenine dinucleotide phosphate (NADP+), 3.3 mM glucose-6-phosphate, 0.4 U/ml glucose-6-phosphate dehydrogenase, 120 μM sodium citrate buffer, and 3.3 mM magnesium chloride (MgCl2) [3, 4]. Microsomes were incubated with uridine 5′-diphospho-glurcuronic acid (UDPGA) cofactor solution A (BD Gentest, Woburn, MA) at a reaction concentration of 2 mM along with solution B (BD Gentest, Woburn, MA); 50 mM Tris–HCl, 8 mM MgCl2, and 25 μg alamethicin in deionized water. p28 was added to individual reaction mixtures to yield a final concentration of 10 μM and reaction mixtures (0.5 ml) incubated in triplicate at 37°C for 0, 5, 15, 30, 60, and 120 min, quenched with 0.1 ml 7% perchloric acid, centrifuged at 12,500 rpm (11,000×*g*) for 5 min, and supernatants transferred to autosampler vials for analysis. The reaction system was validated using a substrate/metabolite-positive control (7-ethoxycoumarin/7-hydroxycoumarin; 7-ethoxycoumarin/7-hydroxycoumarin glucuronide) and four negative control reactions conducted in parallel with each set of substrate reactions: no substrate, quenched microsomes added after quenching, no microsomes, and no cofactor to account for glucuronidation [2].

Metabolism

Metabolites of p28 were separated and identified by LC/MS/MS in supernatants following a 2-h incubation of p28 with liver microsomes using an Applied Biosystems API 4,000 QTrap mass spectrometer with Analyst 1.4.1 software. p28 and its metabolites were separated on an Aquasil 100 × 2 mm column. The HPLC eluent was monitored by electrospray ionization mass spectrometry using: MRM transitions for the quantitative analysis of metabolites, the independent data acquisition mode to trigger enhanced product ion scans and identify potential metabolites based on common or expected biotransformations (e.g., oxidation, hydrogenation) as well as unexpected metabolites (e.g., loss of amino acids), and LightSight software Version 1.1 (Applied Biosystems; Foster City, CA). The mass of the triply charged ion (p28 2914 Daltons; M3+, *m/z* 972) was observed and used to search for potential metabolites. Scans of the reaction samples were compared with the negative control reactions to ensure the observed peaks were not due to the reaction matrix. Potential metabolites were verified by comparing the MS/MS spectra of the potential metabolite to that of the parent.

Metabolites of p28 were also identified in the serum of NHP receiving 60 and 120 mg/kg/day iv for 28 days. Serum samples were collected at 5 min, and 1 and 4 h after administration on day 1 and 22, respectively. Dose- and time-related increases in the amounts of each metabolite were quantified as % of the total peak area of p28 and its potential metabolites measured in serum collected from the respective monkey at 5 min after dosing.

Cell uptake of p28

Human melanoma (Mel-6 p53null, Mel-29 p53wt), HK2 (normal kidney) cells, and fibroblasts were seeded into 25-cm^2 flasks at 5 × 10^5 cell density/cell line and cultured overnight. Cells (1 × 10^6) were washed with culture media, pre-warmed fresh culture media (5% FBS, phenol-red free) containing 100 μM p28, and cells incubated at 37°C under 5% CO_2 for 2, 5, 10, 15, 30 min, 1, and 2 h. The supernatant was removed, cells washed, and incubated with trypsin–EDTA for 2 min, washed again, centrifuged at 1,000×*g* for 2 min, and snap frozen prior to assay for intact p28 by LC/MS/MS [1].

Immunogenicity

Any potential antibody response to p28 was determined in 6- to 8-week-old female BALB/c mice maintained under specific pathogen-free conditions. Mice were distributed randomly into three groups and immunized as follows: Group I with 100 μg/mouse of p28 alone, Group II with 100 μg p28 emulsified in complete (CFA) or incomplete (IFA) Freund's adjuvant (Sigma–Aldrich, USA), and Group III with CFA alone. CFA was used for the initial and IFA for subsequent immunizations. Mice were consecutively immunized for 5 days and then on days 8 through 12 and 15 through 19, bled on days 0, 7, 14, and 21, and serum separated and stored at −20°C. Antibody titers were determined by ELISA using purified p28 (5 μg/ml; 0.1 M carbonate bicarbonate buffer pH 9.6) to coat 96-well microtiter plates (Corning Costar 96-well plate, e-Bioscience, San Diego, CA) overnight at 4°C. The plates were blocked with 200 μl/well 3% BSA in PBS at room temperature for 2 h prior to the addition of serially diluted serum samples (1:200 to 1:25,000 in PBS) and incubation at 37°C for 1 h. After four 100 μl washes, horseradish peroxidase-conjugated (HRPO) goat anti-mouse IgG, IgG_1, IgG_{2a}, or IgG_{2b} (Caltag Laboratories, Burlingame, MA) antibodies diluted 1:2,000 in blocking buffer were added and incubated at 37°C for 1 h, tetramethylbezidine (TMB) substrate solution (e-Bioscience) was added, and color

allowed to develop at room temperature in the dark for 15 min. The reaction was stopped with 1 M HCl and absorbance values measured at 450 nm using a Bio-Rad microplate reader (model 550). Results are expressed as OD values. A potential immune response was also analyzed in serum samples of NHP undergoing a subchronic intravenous toxicity study that received p28 for 4 weeks. ELISA plates (Nunc, Polysorp 96 well) were again coated with 5 μg/ml p28 (100 μl per well) overnight at 4°C, blocked with 200 μl per well of blocking buffer (3% BSA in PBS) at room temperature for 2 h, and serially diluted serum samples (1:10 to 1:1,000; PBS) added to peptide-coated plates incubated at 37°C for 1 h (100 μl per well). After four washes, horseradish peroxidase-conjugated (HRP) goat anti-monkey IgG (Fitzgerald Industries International Inc., Concord, MA) antibodies (1:5,000) were added and incubated at 37°C for 1 h (100 μl per well). TMB substrate was added, allowed to develop, and absorbance values determined at 450 nm. The OD values obtained at a 10-fold dilution were used to calculate mean values per group to compare relative IgG response among the groups receiving increasing doses of p28.

Subchronic intravenous toxicity study in mice

Individually housed mice [Crl:CD1(ICR)] were quarantined for 2 weeks in a temperature-controlled room maintained on a 12-h light/dark cycle prior to administration of p28. All mice had free access to Purina Certified Rodent Diet 5002 (PMI Nutrition International, Inc., Brentwood, MO) and tap water ad libitum. After release from quarantine, animals were assigned to experimental groups using a computer-based randomization procedure that blocks for body weights. Dose concentrations were analyzed by HPLC weekly throughout all toxicity studies. Groups of 20 mice/sex received either three iv injections of vehicle only (Dulbecco's phosphate-buffered saline) or p28 per week (M-W–F schedule) at doses of 60, 120, or 240 mg/kg/dose (180, 360, and 720 mg/m^2/dose, respectively) for 13 weeks. Dose levels were selected on the basis of a preliminary 4-week range-finding toxicity study in mice, and as a multiple of anticipated human doses.

All mice were observed a minimum of twice daily with detailed clinical examinations and body weight and food consumption measured once weekly. Potential neurotoxic effects were assessed with functional observational battery (FOB) evaluations of 5 mice per sex per group during quarantine (pre-test), during weeks 4 and 12, and during the last week of the recovery period. Indirect funduscopic ophthalmic examinations were performed on all study animals during the quarantine period and during the final week of the treatment period.

Blood samples for clinical chemistry and hematology evaluations were collected from each surviving mouse prior to its scheduled necropsy at the end of the treatment period (day 91) or recovery period (day 121). Clinical chemistry assays (blood urea nitrogen [BUN], aspartate aminotransferase, alanine aminotransferase, alkaline phosphatase, glucose, lactate dehydrogenase, cholesterol, creatinine, BUN/creatinine ratio, triglycerides, total protein, total bilirubin, albumin, sodium, potassium, chloride, calcium and inorganic phosphorus) were performed using a Synchron CX5 Clinical Chemistry Analyzer (Beckman Instruments, Brea, CA). Hematology assays (erythrocyte morphology, hemoglobin, hematocrit, mean corpuscular volume, mean corpuscular hemoglobin, mean corpuscular hemoglobin concentration, platelet count, total and differential [absolute and relative] leukocyte count, and absolute and relative reticulocyte count) were performed using an Advia System 120 Hematology Analyzer (Bayer Corp., Tarrytown, NY).

Plasma clearance data were generated from animals in the toxicology study, after dosing on days 1 and 22. Groups of three mice/sex/time point were lightly anesthetized with 70% CO_2/30% air and bled via retro-orbital sinus puncture at 0, 5, 15, and 30 min and 1, 2, 4, 8, and 24 h. Plasma levels of p28 were quantified by LC–MS/MS.

On study day 91, the first 15 mice/sex/group (numerically) were euthanized by CO_2 overdose and subjected to a complete necropsy. All gross lesions plus $\sim$50 tissues per mouse were collected and fixed in 10% neutral buffered formalin. The remaining mice in each group (recovery animals) were held for an additional 30 days without further treatment, then euthanized and necropsied on study day 121. All tissues collected at the end of the dosing period from all mice in the high dose and vehicle control groups were histopathologically evaluated. Histopathologic evaluation of tissues collected from mice in the low and middle dose groups (euthanized on day 91) and from all mice in the recovery groups (euthanized on day 121) were limited to gross lesions and identified target tissues.

Continuous in vivo data from the mouse toxicology study were compared by analysis of variance (ANOVA), followed by post hoc analysis using Dunnett's test for comparisons of multiple treatment groups to a single control group. Comparisons of incidence data were performed using by X^2 analysis or Fischer's exact test. A minimum significance level of $P \leq 0.05$ was used in all comparisons.

Subchronic intravenous toxicity study in non-human primates

Cynomolgous sp. of both sexes were individually housed in a controlled temperature environment under a 12-h light/dark cycle, fed Certified Primate Diet #2055C (Harlan/

Teklad, Madison, WI) watered ad libitum and received fresh fruit and primate diet supplements regularly. After release from quarantine, NHP were randomized to experimental groups and groups of 5 monkeys/sex received three iv injections per week (M–W–F schedule) of p28 (in Dulbecco's phosphate-buffered saline) at doses of 0, 30, 60, or 120 mg/kg/dose (360, 720, and 1,440 mg/m^2/dose, respectively) for 4 weeks. Dose levels of p28 dose used in the subchronic study were selected as a multiple of presumed human doses and to increase doses (on an mg/m^2 basis) beyond those used in mice. All animals were observed a minimum of twice daily, with detailed clinical examinations, body weight, and food consumption measurements performed once weekly. Indirect funduscopic ophthalmic examinations were performed on all study animals during the quarantine period (pre-test) and during the final week of the treatment period. Electrocardiograms (ECGs) were obtained from all monkeys during the quarantine period (pre-test), the final week of the treatment period, and the final week of the recovery period; ECGs were evaluated for heart rate and rhythm, amplitude of the P wave and QRS complex, and duration of the P wave, PR, QRS, and QT intervals.

Blood samples for clinical chemistry, hematology, and coagulation evaluations were collected from all monkeys at pre-test and those designated for necropsy during the final week of the treatment and recovery periods. Animals were fasted a minimum of 12 h prior to collection of blood samples for clinical pathology. Coagulation tests (prothrombin time, fibrinogen, and activated partial thromboplastin time) were performed using an MLA Electra 900 Automatic Coagulation Timer (Hemoliance). Urine samples collected from fasted animals at pre-test, during the final week of treatment, and during the final week of the recovery period were analyzed by dipstick and microscopy.

Pharmacokinetic parameters of p28 in NHP were derived from blood samples collected from the jugular vein of all animals prior to dosing and at 5, 15, and 30 min and 1, 2, 4, 8, and 24 h after dosing on study days 1 and 28. On study day 29, the first 3 monkeys/sex/group (numerically) were euthanized by barbiturate overdose and subjected to a complete necropsy. All gross lesions plus ~50 tissues per animal were collected and fixed in 10% neutral buffered formalin. The remaining two monkeys in each group (designated as recovery animals) were held for an additional 28 days without further treatment and were euthanized and necropsied (as above) on study day 57. Tissues collected from all study animals at the end of the dosing period were histopathologically evaluated, but histopathologic evaluation of tissues collected from monkeys in the recovery groups limited to gross lesions and identified target tissues.

Continuous data from the toxicology study were compared by ANOVA, followed by Dunnett's test. Comparisons of incidence data were compared by X^2 analysis or Fischer's exact test. A minimum significance level of $P \leq 0.05$ was used in all comparisons.

Efficacy

Tumor cells were injected sc (10^6/mouse) in the right flank of 5- to 6-week-old male and female athymic mice as described [5]. When a palpable tumor (3 mm diameter) appeared, animals were computer randomized into control (20 mice) and treatment (10 mice) groups, and injected ip with DTIC, 4 mg/kg bw ip, 3×/week, paclitaxel 12.8 mg/kg (1.5 μmol/l) bw ip on days 10,14,21,25, 5-FU 20 mg/kg bw ip (15.3 μmol/l) on days 4,8,12, or p28 5, 10 or 20 mg/kg bw ip (1.7, 3.4, 6.8 μmol/l) daily for 28 days. Animals were weighed 3×/week, tumor volume (tv) determined [5] and normalized to mean animal body weight. Tumor growth was analyzed by univariate and multivariate statistical methods. Means and standard errors for each day were determined for each group of animals, which were used to generate growth curves. Significance tests to determine differences between the doses and control on day 30 (end of experiment) included parametric (F, t tests) and nonparametric (Kruskal–Wallis, Wilcoxon) methods. Mixed linear model analyses were also conducted to estimate growth over the entire longitudinal dataset using log volume as the response. All data were analyzed using SAS. Mice were killed, tumors dissected, freed of fat, weighed, and fixed overnight in formalin-free HIC Zinc fixative for histopathology.

Results

Stability and metabolism

Composite calibration curves prepared with mouse serum evaluated over a concentration range of 100–10,000 ng/ml of p28 showed correlation coefficients of 0.9962 and 0.9976 on day 1 and day 22, respectively. Mean percent accuracy values ranged from 91.6 to 105%, with coefficients of variation less than 12%. The concentrations of p28 measured in mouse serum samples spiked with p28 at concentrations higher than the ULOQ, and dilutions intended to fall within the range of the standard curve were within 15% of the theoretical concentration. Cross-validation of the analytical method for mouse, dog, NHP, and human serum demonstrated that the inter-day accuracy ranged from 90 to 109% and inter-day precision (CV %) ranged from 0.87 to 14% for p28 in serum from the four species. The mean recovery (0.2, 1, and 5 μg/ml) of p28

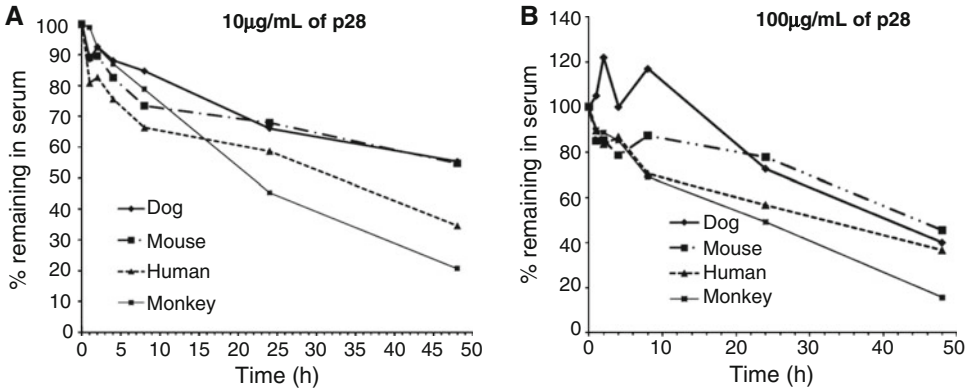

Fig. 1 Stability of p28 in the serum of dog, human, mouse, and NHP. **a** 10 µg/ml = 3.4 (µmol/l) p28. **b** 100 mg/l = 34.3 (µmol/l) p28

from mouse serum was 96.4%; human, 95.4%; dog, 87.5%; and NHP, 87.9% setting the lower limit of quantitation at 100 ng/ml [1].

p28 stability in serum

Although p28 was stable in mouse serum extracts through at least three freeze thaw cycles, its stability in serum was affected by temperature. In general, p28 was resistant to hydrolyzation at 4°C for up to 48 h without significant degradation. At 4°C, there was minimal (<30%) degradation of p28 in mouse, dog, NHP, or human serum over a 48-h incubation period, while incubation of 10 µg/ml (~3.3 µM) p28 at 37°C with mouse, dog, monkey, and human serum for up to 48 h resulted in 45, 45, 79, and 65% degradation of p28, respectively (Fig. 1a). Similar results were observed when the concentration of p28 was increased to 100 µg/ml (Fig. 1b), suggesting enzymatic processes are involved in the metabolism of p28.

p28 stability in liver microsomes

The viability of the microsomal reaction system was confirmed by loss of 7-ethoxycoumarin (*m*/*z* 191) and formation of 7-hydroxycoumarin (7-OHC, *m*/*z* 163) and 7-OHC glucuronide (*m*/*z* 339), as detected in Q1 scans in positive ion mode. 7-Ethoxycoumarin (7-EC) is metabolized by phase I enzymes to produce 7-hydroxycoumarin (7-OHC, *m*/*z* 163), and the latter can undergo phase II glucuronide conjugation. p28 (10 µM) was most stable (41.4%) in human liver microsomes, with 19.3 and 10.3% remaining in mouse and NHP microsomes after 120 min, respectively (Table 1).

p28 metabolites identified in vitro

The enhanced MS and product ion scans for p28 showed 5 potential metabolites from human liver microsomes and 4 from mouse and NHP liver microsomes, respectively

Table 1 Stability of p28 in mouse, NHP, and human liver microsomes

Time (min)	% p28 remaining		
	Human	Mouse	NHP
0	100	100	100
5	98.8	92.2	91.9
15	91.6	78.0	77.2
30	67.0	56.8	51.0
60	56.7	37.5	26.3
120	41.4	19.3	10.3

(Table 2). In human liver microsomes, oxidation of p28 accounted for 36.4% of total peak area. After 2-h incubation, the predominant metabolite was loss of the N-terminal leucine from p28 (M2) that appeared 62.8, 62.8, and 11.7% in all mouse, monkey, and human liver microsomes, respectively, after 2 h followed by loss of Leu-Ser-Thr from the N-terminal of the peptide (M5) in all species of liver microsomes. Loss of Leu-Ser-Thr-Ala (M6) accounted for 10% of total peak area in liver microsomes from NHP (Table 2).

p28 metabolites identified in vivo

Serum samples collected for analysis following iv administration to NHP were quantitatively analyzed based on the percent of total peak area of p28 and its individual metabolites. The predominant metabolite observed on day 1 was the loss of the N-terminal leucine (M2). The percentage of this metabolite observed on day 22 was decreased with respect to the percentage observed on day 1. The predominant metabolite observed on day 22 was the oxidation product of p28, similar to that observed in the reference standards prepared with the samples reflecting a combination of metabolism and degradation of p28 (data not shown). Quantitative analysis of the peak area revealed that 5 min after iv administration, the average amounts

Table 2 Relative quantitation (% of total peak area) of major metabolites of p28 (10 μM) at the end of 2-h incubation at 37°C with mouse (MLM), monkey (KLM), and human (HLM) liver microsomes, respectively

p28, Leu-Ser-Thr-Ala-Ala-Asp-Met-Gln-Gly-Val-Val-Thr-Asp-Gly-Met-Ala-Ser-Gly-Leu-Asp-Lys-Asp-Tyr-Leu-Lys-Pro-Asp-Asp

ID	Found (*m/z*; 3+)	Possible structures	% total area in MLM	% total area in KLM	% total area in HLM
p28	972		23.4	12.7	40
M1	977.4	Oxidation			36.4
M2	934.6	Loss of Leu	62.8	62.8	11.7
M3	939.7	Loss of Leu + oxidation			7.2
M4	905.8		3.2		
M5	871.8	Loss of Leu-Ser-Thr	3.8	8.8	3.4
M6	847.8	Loss of Leu-Ser-Thr-Ala		10.1	
Others			6.8	5.6	1.4

Table 3 Relative percent (%) of p28 and its major metabolites formed following iv administration of p28 (60 and 120 mg/kg/day) to NHPs ($n = 5$ per sex)

Metabolites	Male					Female				
	p28	M1	M2	M5	M6	p28	M1	M2	M5	M6
60 mg/kg										
Day 1, 5 min	80.6	4.0	11.5	1.2	0.5	78.4	3.6	14.3	1.04	0.51
Day 1, 1 h	1.5	0.2	0.3	0.0	0.0	1.3	0.2	0.3	0.0	0.0
Day 22, 5 min	86.8	4.5	5.6	1.0	0.4	90.0	2.7	4.8	0.9	0.4
Day 22, 1 h	2.8	0.2	0.3	0.0	0.0	1.9	0.2	0.2	0.0	0.0
120 mg/kg										
Day 1, 5 min	71.5	4.7	19.0	2.2	0.74	72.8	4.5	18.3	1.8	0.7
Day 1, 1 h	1.5	0.2	0.4	0.0	0.0	2.0	0.2	0.4	0.0	0.0
Day 22, 5 min	83.3	5.0	8.4	1.2	0.5	86.8	3.9	6.2	1.2	0.6
Day 22, 1 h	4.0	0.2	0.3	0.1	0.0	3.8	0.3	0.4	0.1	0.0

The amount of each metabolite was taken as % of the total peak area of p28 in serum collected at 5 min after dosing

($n = 5$) of M2 and M5 were 11.5 and 1.2%. The amount of intact p28 with time following iv injection of 120 mg/kg p28 to male *Cynomolgous* sp. is shown in Table 3.

Cellular uptake of p28 in vitro

Figure 2 illustrates the intracellular concentration of intact p28 in human $p53^{null}$ Mel-6 and $p53^{wt}$ Mel-29 melanoma and human kidney HK2 cells over a 2-h time course of exposure. Although cleared almost exclusively by the kidney, cellular uptake is rapid and preferential in cancer cells [7]. In contrast, entry of p28 into fibroblasts was essentially at the level of (quantifiable) assay sensitivity (100 ng/ml). p28 appears to be retained at significantly higher levels in p53 positive cells, where p28 binds to p53 in the cell nucleus [10], confirming initial confocal and

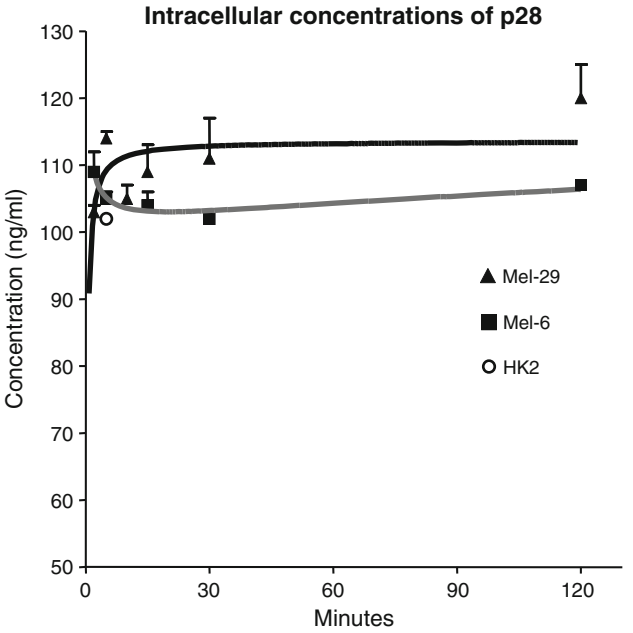

Fig. 2 Intracellular concentrations of intact p28 in cancer and normal cell lines with time (min) after exposure. 120 ng-p28/ml = 41.2 (nmol/l) = 0.042 (μmol/l)

cytometric analyses that suggest p28 entry is maximal 2-h post-exposure, but is retained longer in cancer cells positive for p53 [7].

Immunogenicity

There was no significant increase in murine IgG levels following immunization with p28. The titers of anti-p28 antibodies were not significantly different between Groups I, II, and III, and there was no correlation between the number of immunizations nor with the use of adjuvant. There was also no significant difference between the levels of IgG_1, IgG_{2a}, and IgG_{2b}. In sum, p28 did not induce any significant alteration in circulating IgG levels or alterations in IgG isotype (ELISA) 7, 14, and 21 days post id administration of p28 in BALB/c 6- to 8-week-old female mice with or without CFA (Fig. 3). IgG values for

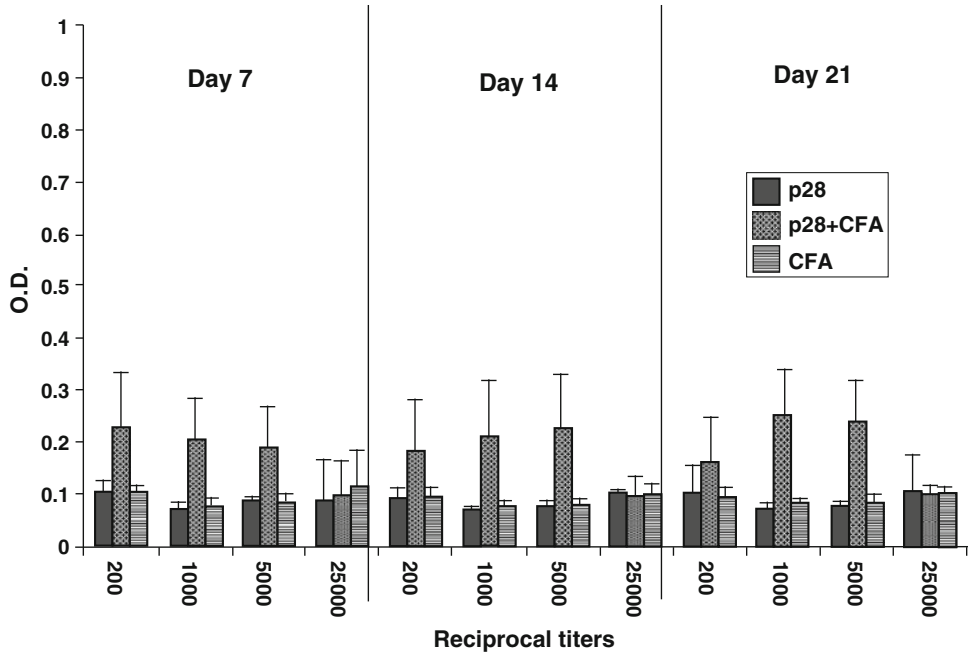

Fig. 3 IgG titers in sera of mice immunized with p28 with and without CFA, and CFA alone. Mice were bled on days 0, 7, 14, and 21 post injection id. Serum samples were diluted 1:200 to 1:25,000

p28-treated groups of NHP were not significantly different from those obtained for untreated animals irrespective of sex (Fig. 4a, b). Although sample to sample variation was present, the average group OD values were not significantly correlated with either the iv dose of p28 or duration after immunization and represent non-specific binding, as similar values were noted in non-immunized animals where the average OD values at 1: 100 fold dilution were negligible. This indicates that p28 did not induce a significant IgG response in *Cynomolgous* sp.

Thirteen-week intravenous toxicity study (with recovery) of p28 in mice

No p28-related deaths were observed. p28 did produce a dose-related decrease in male mean total body weight gain, while female mean total body weight gain increased with dose, but the total weight gained for p28-treated mice during the entire study was comparable to the respective control groups. Necropsy findings included an enlarged spleen in one of 15 female mice receiving 60 mg/kg and mottled lungs for 1/15 males receiving 120 mg/kg. Although sporadic ophthalmic lesions were noted in the mice, these lesions occurred incidentally in untreated mice and were not dose related. No other lesions were noted for these animals. All animals behaved normally with no treatment-related clinical signs noted during the study. At terminal necropsy, adrenal (240/mg/kg), heart (60, 120, 240 mg/kg), and thymus (60, 120, 240 mg/kg) weights were statistically decreased in males, but reversible within 28 days following cessation of dosing (recovery). Thymus weight significantly increased in female animals receiving

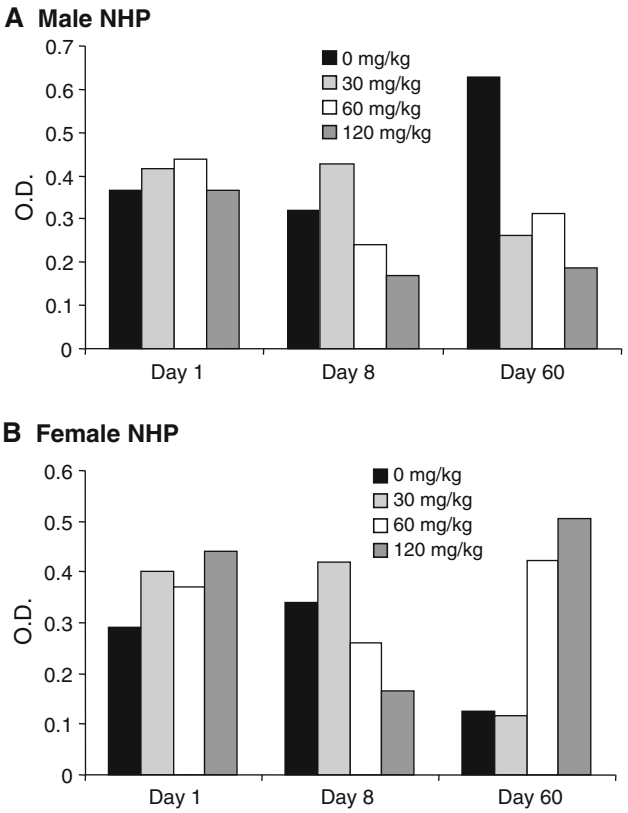

Fig. 4 Lack of immune response to increasing doses of p28 injected iv in **a** male and **b** female NHP (*Cynomolgous* sp.). 30 mpk = 10.2 (μmol/l); 60 mpk = 20.4 (μmol/l); 120 mpk = 40.8 (μmol/l)

240 mg/kg at recovery necropsy. Although the effects of p28 on organ weight appear treatment related, histopathologic evaluation of tissues in mice receiving 240 mg/kg

and control groups failed to exhibit any pattern of toxicity associated with p28, and no tissues were identified as targets of p28 toxicity. No treatment-related or toxicologically significant effects on body weights, food consumption, ophthalmology, FOB, clinical chemistry, and hematology were observed during the study. The no observed adverse effect level (NOAEL) for female mice was 120 mg/kg/dose as the only effects noted (increased thymus weight) were seen at the highest p28 dose. As a result of the decreased heart and thymus weights in male mice in all dose groups, a NOAEL could not be defined. The lack of limiting toxicity at the highest dose (240 mg/kg/dose) suggests the maximum-tolerated dose (MTD) for 3× week administration of p28 for 13 weeks is ≥240 mg/kg/dose (720 mg/m^2/dose).

Four-week intravenous toxicity study (with recovery) of p28 in NHP

Cynomolgous sp. (five monkeys/sex/group in 4 Groups) were dosed with 30, 60, and 120 mg/kg/p28 iv 3× per week for four consecutive weeks, followed by a 4-week recovery period. A detailed histopathological evaluation was done on all animals killed at the end of the 4-week treatment period. No animals died or were killed moribund during the study, no treatment-related clinical signs of toxicity, or evidence of any ocular toxicity, cardiotoxicity, neurotoxicity, or immunotoxicity were observed, and there were no treatment-related effects on body weights, body weight gain, food consumption, clinical pathology (clinical chemistry, hematology, coagulation parameters, and urinalysis), or organ weights. No treatment-related gross abnormalities or microscopic changes were observed at necropsy in any animal. The NOAEL following iv administration of p28 at 30, 60, and 120 mg/kg three times per week for four consecutive weeks to male and female cynomolgous was 120 mg/kg (1,440 mg/m^2), with the MTD for *Cynomolgous* sp. ≥120 mg/kg (1,440 mg/m^2/dose).

Pharmacokinetic analysis of p28 in mice

Pharmacokinetic data were fit to a two (30 or 120 mg/kg) or three (480 mg/kg) compartment model and subjected to non-compartmental analysis. The pharmacokinetic parameters of p28 in serum following a single iv injection is presented in Table 4. The concentration-related parameters AUC and Cmax increased proportionally with dose, with the AUC of p28 being 13.9, 65.7, and 278 h μg/ml for mice receiving 30, 120, or 480 mg/kg, respectively. The apparent half-life of the α-phase (distribution) and β-phase (elimination) was similar within phase across dose levels, suggesting that the pharmacokinetics of p28 do not change with dose. At the highest dose (480 mg/kg), a prolonged γ-phase of elimination of 34.1 h was observed for p28, which may contribute to the large volume of distribution (Vdss) obtained at high concentrations of p28.

Table 4 Pharmacokinetic parameters calculated from plasma concentrations of p28 following a single iv dose to mice[a]

Parameter	Dose (mg/kg iv)		
	30	120	480
Cmax (μg/ml)	129	589	2,473
Tmax (h)	0.033	0.033	0.033
$t_{1/2\alpha}$ (h)	0.06	0.02	0.03
$t_{1/2\beta}$ (h)	0.40	0.25	0.23
$t_{1/2\gamma}$ (h)	NA	NA	34.1
AUC_{0-t} (h·μg/ml)[b]	13.9	65.7	278
Clearance (ml/kg/h)[b]	2,159	1,825	1,727
Vdss (ml/kg)	297	167	4,084

[a] Parameters were calculated from compartmental analysis of the data, except where indicated

[b] Calculated from non-compartmental analysis of the data

Pharmacokinetic analysis of p28 in NHP

Serum concentrations of p28 increased directly with dose and were similar on day 1 and day 22 of treatment when NHP were injected iv 3× week for 4 weeks. Mean AUC last values also increased with increasing dose, and on day 1 were 27.4, 53.6, and 117 h μg/ml for males and 39.4, 54.0, and 117 h μg/ml for females given 30, 60, or 120 mg/kg/day, respectively. The mean terminal elimination half-life of p28 in serum was similar at increasing dose levels ranging from 0.33 to 0.50 h, suggesting p28 exhibits linear kinetics in mice and NHP irrespective of sex (Fig. 5; Table 5).

Efficacy

p28 produced significant dose-related decreases in the proliferation of HCT-116 (colon), UISO-Mel-23 (melanoma) and MDA-MB-231 (breast) xenografts (Fig. 6) with a range (1.7–6.8 μmol/l) of doses, equally effective in HCT-116 xenografts, suggesting lower doses might be equally effective. p28 also produced a dose-related decrease in the growth of UISO-Mel-23 and MDA-MB-231 xenografts (which overexpress p53), with the highest dose of p28 (10 mg/kg bw; 3.4 μM) as effective as either DTIC or paclitaxel administered at a dose that produced an average 20% decrease in body weight but no mortality. These studies suggest that a 10 mg/kg bw (3.4 μmol/l) dose of p28 provides a starting point for efficacy in a human trial in patients with solid tumors that express either wild type or mutated (overexpressing) p53.

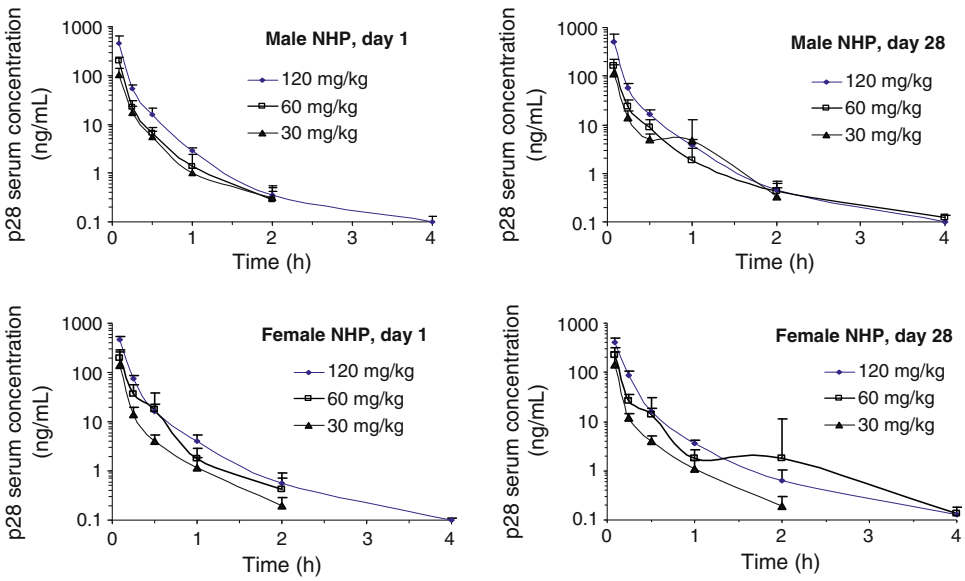

Fig. 5 Clearance of increasing concentrations of p28 following administration of a single dose to male/female NHP (*Cynomolgous* sp.). 100 ng-p28/ml = 0.0343 (μmol/l)

Discussion

The pharmacokinetic and metabolic profiles of p28 in mouse, human, and NHP hepatic microsomes and serum were determined by Quantitative HPLC/MS/MS [1]. In mice, mean serum levels of p28 increased in proportion to the increase in iv dose level and were 129, 589, or 2,473 μg/ml (or 44.3, 202.3, and 848.7 μmol/l, respectively) at 0.033-h post iv administration of 30, 120, or 480 mg/kg, respectively (toxicity study). The apparent serum half-life of the β-phase of elimination of p28 was similar over the three dose levels and ranged from 0.23 to 0.40 h with a prolonged elimination phase only observed in mice receiving 480 mg/kg of p28. During an earlier range-finding toxicity study, analyses of serum samples in mice receiving 60, 120, or 240 mg/kg/day p28 iv three times a week for 13 weeks also established that serum concentrations of p28 increased with increasing dose levels and exhibited linear kinetics with increasing dose.

Analyses of serum samples in male and female NHP receiving 30, 60, or 120 mg/kg/day p28 iv three times a week for 4 weeks also indicated that serum concentrations of p28 and AUC last values increased with increasing dose level, with the mean terminal elimination half-life in serum similar across dosage groups. p28 exhibited linear kinetics in NHP, with no apparent differences in pharmacokinetics between day 1 and day 22, irrespective of sex, suggesting that the elimination and distribution of p28 did not change following repeated dose administration. However, although the metabolism of p28 in NHP showed that the predominant metabolite on day 1 was the loss of the N-terminal leucine from the peptide, on day 22, the percentage of this metabolite in serum was lower than observed on day 1, with the predominant metabolite being the oxidation product of p28. While not yet translatable to humans, the results suggest that the metabolism of p28 in NHP may change with repeated administration in spite of relatively similar kinetics and distribution but that any species difference in the metabolism of p28 may be marginal.

The second major route of metabolism of p28 in humans is via loss of the n-terminal leucine (M2). The rapid uptake and slow intracellular clearance of p28 due to binding in the cell nucleus [7, 10] suggest that a robust amount of mature p28 or the M2 metabolite enters a cancer cell in spite of the relatively rapid oxidation in the circulation and effects a response [10]. We have recently reported that although the c-terminal end of p28, aa 67–77 of azurin or p12, is involved in the binding of p28 to p53, loss of the n-terminal or α-helical end of the peptide results in a loss of preferential entry into cancer cells [7, 10]. The increased intracellular accumulation of p28 in p53 wt Mel-29 over p53 null Mel-6 cells (Fig. 2) supports this observation. Peak serum levels of intact p28 in mice and NHP closely approximate the concentration observed intracellularly and those required to establish and effective response.

In summary, p28 appears as a stable peptide with a dose dependent, rapid to intermediate clearance in mice, rats, dogs, and monkeys that distributes extensively in these species and has no effect on circulating IgG isotypes IgG_1, IgG_{2a}, and IgG_{2b} in mice and NHP, irrespective of sex, or on food consumption and clinical or anatomic pathology that were not reversible during recovery. When coupled with a sequential series of metabolites originating from the n-terminus of the peptide that leaves an active, therapeutic portion of the molecule [10] circulating intact over a longer period of time, the peptide offers an excellent opportunity to effect a clinical response in patients expressing p53 wt or mutant tumors. Overall, preclinical investigation of the

Table 5 Pharmacokinetic parameters of p28 on days 1 and 22 during the consecutive 4-week iv administration (3×/week) to NHPs ($n = 5$ per sex/dose)

Parameters	Dose											
	30 mg/kg				60 mg/kg				120 mg/kg			
	Male		Female		Male		Female		Male		Female	
	Day 1	Day 22	Day 1	Day 22	Day 1	Day 22	Day 1	Day 22	Day 1	Day 22	Day 1	Day 22
Csmin (~g/ml)	103 ± 39	113 ± 61	143 ± 117	147 ± 110	203 ± 33.0	163 ± 56	195 ± 85.7	229 ± 86.8	447 ± 195	503 ± 243	454 ± 92	416 ± 74.1
$t_{1/2}$ (h)[a]	0.33 ± 0.03	0.48 ± 0.12	0.42 ± 0.23	0.41 ± 0.22	0.35 ± 0.15	0.73 ± 0.32	0.42 ± 0.21	0.70 ± 0.16	0.50 ± 0.18	0.51 ± 0.18	0.49 ± 0.21	0.52 ± 0.17
AUClast (h g/ml)[b]	27.4 ± 10.1	32.5 ± 19.7	39.4 ± 34.6	41.5 ± 32.9	53.6 ± 9.2	44.0 ± 16.2	54.0 ± 24.3	67.4 ± 31.7	117 ± 53	133 ± 64.1	117 ± 23.2	107 ± 19.0
Clearance (ml/hr/kg)[c]	1,209 ± 414	1,141 ± 483	1,297 ± 903	1,201 ± 864	1,150 ± 229	1,482 ± 434	1,367 ± 734	1,079 ± 523	1,160 ± 378	1,061 ± 432	1,056 ± 180	1,143 ± 200
Vdss (ml/kg)[d]	202 ± 79	219 ± 79	202 ± 175	188 ± 193	136 ± 43	276 ± 93	244 ± 162	268 ± 227	154 ± 70	153 ± 95.7	153 ± 41	189 ± 48.3

[a] Half-life of the terminal elimination phase

[b] Area under the serum concentration versus time curve calculated from 0 to the last time point the concentration of p28 in serum was above the reliable level of quantitation

[c] Total body clearance

[d] Volume of distribution at steady state

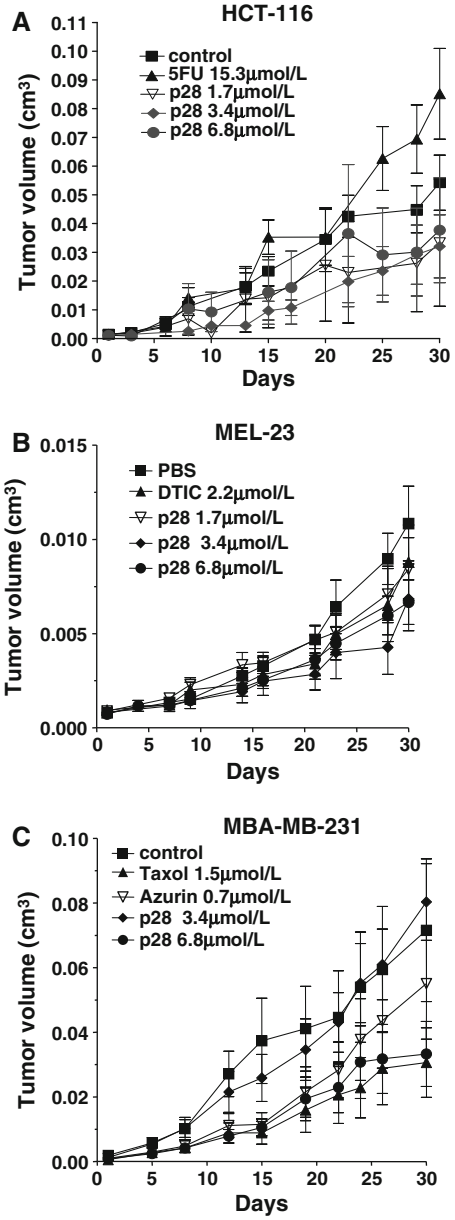

Fig. 6 Efficacy of p28 in: **a** human colon (HCT-116; p53wt), **b** melanoma (Mel-23; p53 mut), and **c** breast cancer (MDA-MB-231; p53mut)

pharmacokinetics and in vivo efficacy of p28 demonstrates a close relationship between human pharmacokinetics and efficacy, suggesting the data appear useful to predict therapeutic dose levels in clinical trials.

Acknowledgments Research supported by CDG Therapeutics, the NCI RAID program and by NCI N01-CM-52203.

References

1. Gorman GS, Coward LU, Freeman L, Noker PE, Beattie CW, Jia L (2010) A novel and rapid LC/MS/MS assay for bioanalysis of

azurin p28 in serum and its pharmacokinetics in mice. J Pharm Biomed Anal 53:991–996
2. Jia L, Liu X (2007) The conduct of drug metabolism studies considered good practice (II): in vitro experiments. Curr Drug Metab 8:822–829
3. Jia L, Noker PE, Coward L, Gorman GS, Protopopova M, Tomaszewski JE (2006) Interspecies pharmacokinetics and in vitro metabolism of SQ109. Br J Pharmacol 147:476–485
4. Jia L, Noker PE, Piazza GA, Leuschner C, Hansel W, Gorman GS, Coward LU, Tomaszewski J (2008) Pharmacokinetics and pharmacodynamics of Phor21-betaCG(ala), a lytic peptide conjugate. J Pharm Pharmacol 60:1441–1448
5. Punj V, Bhattacharyya S, Saint-Dic D, Vasu C, Cunningham EA, Graves J, Yamada T, Constantinou AI, Christov K, White B, Li G, Majumdar D, Chakrabarty AM, Das Gupta TK (2004) Bacterial cupredoxin azurin as an inducer of apoptosis and regression in human breast cancer. Oncogene 23:2367–2378
6. Rauth S, Kichina J, Green A, Bratescu L, Das Gupta TK (1994) Establishment of a human melanoma cell line lacking p53 expression and spontaneously metastasizing in nude mice. Anticancer Res 14:2457–2463
7. Taylor BN, Mehta RR, Yamada T, Lekmine F, Christov K, Green A, Bratescu L, Shilkaitis A, Chakrabarty AM, Beattie CW, Das Gupta TK (2009) Noncationic peptides obtained from azurin preferentially enter cancer cells. Cancer Res 69:537–546
8. Yamada T, Fialho AM, Punj V, Bratescu L, Gupta TK, Chakrabarty AM (2005) Internalization of bacterial redox protein azurin in mammalian cells: entry domain and specificity. Cell Microbiol 7:1418–1431
9. Yamada T, Hiraoka Y, Ikehata M, Kimbara K, Avner BS, Das Gupta TK, Chakrabarty AM (2004) Apoptosis or growth arrest: modulation of tumor suppressor p53's specificity by bacterial redox protein azurin. Proc Natl Acad Sci USA 101:4770–4775
10. Yamada T, Mehta RR, Lekmine F, Christov K, King ML, Majumdar D, Shilkaitis A, Green A, Bratescu L, Beattie CW, Das Gupta TK (2009) A peptide fragment of azurin induces a p53-mediated cell cycle arrest in human breast cancer cells. Mol Cancer Ther 8:2947–2958